Using virtual input rejection to improve control of a platform for characterizing the mechanical properties of human oocytes

Joël Abadie[1], Sylvain Hernandez-Sabio[1], Emmanuel Piat[1]

***Abstract*— Mechanical characterization of human oocytes holds great promise for improving the chances of pregnancy in assisted reproduction programs. However, the development of a high-performance device comes up against the numerous biological and normative constraints of medically Assisted Reproduction Technology (ART). The patented EggSense platform overcomes these difficulties and enables the mechanical characterization of human oocytes under clinical conditions. In this article, the focus is on the significant improvements achieved in EggSense by deploying advanced control techniques, based on Virtual Input Rejection COntrol (VIRCO). This approach is used to control the position of the force-sensing element in contact with the oocyte. Its implementation is fully described and experimentally validated. A comparison with a conventional controller is also provided to illustrate some of the benefits of VIRCO.**

I. Introduction

Characterization of oocyte mechanical properties is a promising research field to improve Assisted Reproduction Techniques (ART). Indeed, according to Yanez et al. the developmental potential of a human oocyte can be predicted by its mechanical properties [1]. Measurements of these properties could represent a significant advance for in vitro fertilization (IVF) procedures, as they would provide an objective criterion to improve oocyte sorting and thus IVF success rates. Nevertheless, such characterization begs the question of the measurement of micro/nano forces in accordance with ART biological constraints. Industrial instruments such as atomic force microscopes or nanoindenters, as well as research prototypes, enable measurement of forces at nano and micronewton scales. Some of these have been used to study the mechanical properties of oocytes [2]. The development of such platforms capable of measuring microforces is complex, and extracting mechanical properties from human oocytes is challenging due to their small size (diameter between 110 and 150 μm) and highly variable stiffness. In addition, a platform dedicated to oocyte characterization must meet specific ART-related requirements to be used under clinical conditions, such as sterility, cytotoxicity, embryotoxicity, and being a single-use medical device. In 2017, an innovative nanoforce sensing platform was developed to fully complied these requirements thanks to the use of *unstable* magnetic springs [3]. Oocyte stiffness is measured by indentation and, during measurements, the magnetic unstable indenter is automatically stabilized by the reaction force generated by the oocyte on the indenter. This invention, called EggSense, is protected by patent WO2018172688 and received authorization in 2024 from French authorities to be used in a hospital as part of a clinical trial on patients resorting to IntraCytoplasmic Sperm Injection (ICSI).

EggSense indentation technology is based on the use of a glass cylindrical magnetic indenter which is placed in a Petri dish filled with a culture medium (see Fig. 1). External magnetic forces provided by two coils and two M_1 magnets levitate the indenter, and the very low stiffness of the magnetic spring generated is used for subsequent force measurement. The oocyte is transferred to the Petri dish and placed in front of the indenter using a holding pipette. Mechanical characterization of the oocyte is based on loading and unloading phases at constant speed, revealing the force-displacement relationship which proves to be representative of its mechanical behavior [4]. A camera connected to a microscope is placed above the Petri dish to measure the displacement of the indenter. Active control of the unidirectional indenter position is implemented to precisely follow the user-defined ramp input sequences during the loading and unloading phases.

This paper focuses on the controller implemented within the platform and compares it to a PID controller. The latter is designed from the identified parameters of a linear model of the system dynamics. This more traditional approach is suitable for many industrial prototypes, but several problems arise when applied to this particular system. Indeed, PID tuning parameters must be adjusted for each oocyte to be characterized, due to the significant variability of oocyte stiffness within the same cohort, which has a direct impact on indenter dynamics. Moreover, the indenter stability vanishes every time the contact with the oocyte is lost, which cannot be handled by

*This work has been achieved in the frame of the EIPHI Graduate school (contract "ANR-17-EURE-0002") and was funded by SATT-Sayens and French National Research Agency (ANR) project number ANR TRAFALDA (N° ANR-23-CE42-0022).

[1]Université Marie et Louis Pasteur, SUPMICROTECH, CNRS, institut FEMTO-ST, F-25000 Besançon, France joel.abadie@femto-st.fr, sylvain.hernandez2@femto-st.fr, emmanuel.piat@ens2m.fr

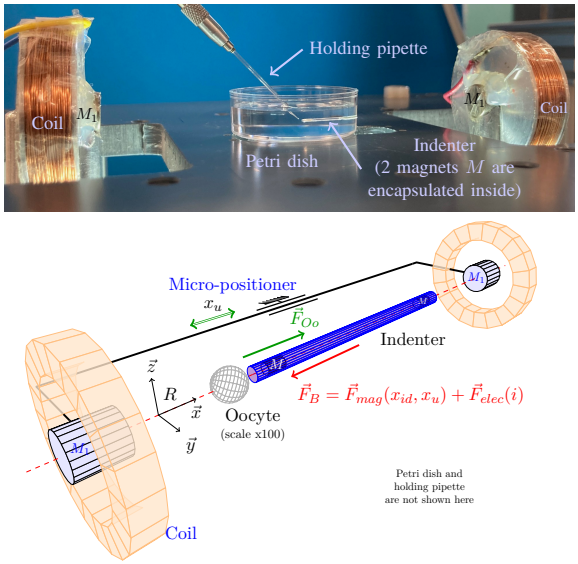

Fig. 1. Overview of the EggSense platform indenter. The oocyte is maintained by an ICSI holding pipette. The indenter is levitating in the culture medium in front of the oocyte. The magnetic field is generated by the two external moving magnets M_1 and coils.

a traditional PID controller. These are the reasons why Virtual Input Rejection COntrol (VIRCO) is implemented on this platform. This approach can be seen as an extension of Active Disturbance Rejection Control (ADRC) framework [5], and has been first used to control the position of a 2DOF piezoelectric cantilever [6]. It relies on the equivalent representation of an uncertain nonlinear system using an approximate linear model and an additive virtual input. An estimate of this virtual input is calculated using an unknown input observer, and is then used to achieve a global linearization of the uncertain nonlinear system. The underlying theory of this approach was initially introduced by Amokrane et al. in 2021 [7] and extended by Hernandez et al. in 2025 [8]. This paper presents the complete implementation of VIRCO controller on the EggSense platform. Experimental results are provided to illustrate the robustness of this method to the variability of oocyte mechanical properties.

II. Indenter Dynamics Modeling

As illustrated in Fig. 1, the indenter is a rigid body of mass m equal to 8 mg that levitates in the culture medium thanks to the magnetic field created by two external magnets M_1. This rigid body is a sealed glass capillary, 1.6 cm long and 0.8 mm in diameter, with two small cylindrical magnets, 0.5 mm in diameter, encapsulated near the ends. These four magnets are aligned along the $\vec{x}$ direction according to this arrangement NS [NS NS] NS, N and S being respectively the north and south magnetic poles and the square brackets representing the indenter ends. This magnetic configuration restricts the displacement of the indenter and ensures its alignment along the measurement direction $\vec{x}$. Indeed, the indenter is aligned along the lateral direction $\vec{y}$ and $\vec{z}$ by the permanent magnetic field. The oocyte must be manually placed into the correct position directly in front of the indenter tip. The other DOFs are therefore neglected, which justifies the mechanical modeling of the indenter dynamics along the $\vec{x}$ direction of the fixed vision reference frame of the camera $R(\vec{x}, \vec{y}, \vec{z})$ [3].

The indenter is subjected to an external force $\vec{F}_B$ which is the sum of the magnetic interaction force $\vec{F}_{mag}$ with the two magnets M_1, and the electromagnetic interaction force $\vec{F}_{elec}$ with two external coils. Each couple (M_1, coil) is fixed on a rigid frame mounted on a micropositioner. Since the indenter dynamics is unstable along $\vec{x}$ without the oocyte, there exists an unstable equilibrium position x_u centered between the two magnets M_1, where $\vec{F}_{mag}$ is zero. The unstable magnetic spring that describes the interaction force $\vec{F}_{mag}$ is thus defined as:

$$F_{mag} = -K_m \left(x_{id} - x_u\right) \tag{1}$$

with K_m the stiffness of the magnetic spring which is negative and x_{id} the indenter coordinates along $\vec{x}$. The coils are placed in a Maxwell configuration, which means that the force $\vec{F}_{elec}$ generated for a given current i injected into the coils is not correlated with the position of the indenter, but only depends on the positive electrical stiffness K_e, so that

$$F_{elec} = K_e\, i. \tag{2}$$

Finally, $\vec{F}_{Oo}$ represents the reaction force applied by the oocyte on the indenter along $\vec{x}$, and thus corresponds to an unknown scalar input. The force value F_{Oo} is estimated using an Extended State Linear Kalman Filter (ES-LKF) [9], which is not detailed here. The physical law governing $\vec{F}_{Oo}$ is difficult to express analytically, but its experimentally observed evolution depends on both the indentation depth d_{Oo} related to the displacement x_{id} of the indenter and the stiffness of the oocyte, which vary significantly over time due to changes in its internal structure. Measurements performed with EggSense show that these stiffness variations are mostly between 0.006 N/m and 0.05 N/m. Therefore, the coupling between the indenter (a rigid body) and the oocyte (a deformable body) leads to an uncertain and non-stationary complex system due to the unknown force $\vec{F}_{Oo}$. However, this force stabilizes the indenter dynamics as soon as the contact with the oocyte is established ($F_{Oo} \neq 0$). This dynamical behavior can then be described by the following ordinary differential equation, written in the reference frame R along $\vec{x}$ taking into account the friction of the

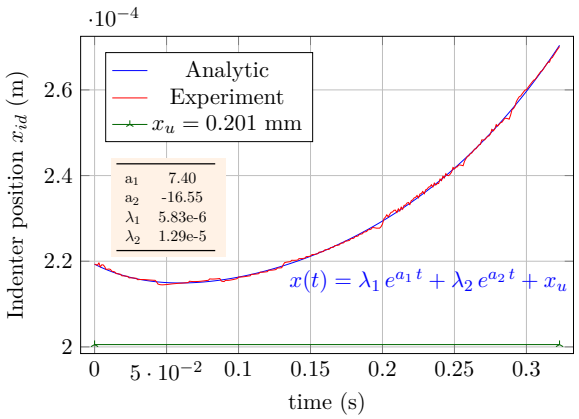

Fig. 2. Open loop free response of the indenter without oocyte. First, the indenter is placed to the left of the viewing zone with VIRCO enabled. The coordinate x_u must be to the left of x_{id} to ensure that the indenter moves to the right when VIRCO is disabled. Position x_{id} is captured until the indenter is stopped by the edge of the Petri dish.

indenter moving through the culture medium:

$$m\,\ddot{x}_{id} + \underbrace{K_v\,\dot{x}_{id}}_{-friction} + \underbrace{K_m(x_{id}-x_u)}_{-F_{mag}} = \underbrace{K_e\,i}_{F_{elec}} + \underbrace{F_{Oo}}_{Oocyte}. \tag{3}$$

This second-order model takes the unstable equilibrium position x_u as a parameter, considers the current i and displacement x_{id} as the control input and system output respectively, and is disturbed by an additional unknown input F_{Oo}.

The mass value is determined using a precision balance. The coefficients K_v and K_m are determined using the unstable free response of the indenter. To observe the latter, closed-loop control is first enabled to keep the indenter in a given position. No oocyte is held by the pipette, so the force $\vec{F}_{Oo}$ is zero. The unstable equilibrium position x_u is determined in the reference frame R by monitoring the average control current while moving the magnets and the coils attached to the micropositioner. Indeed, the position of the indenter x_{id} is equal to x_u in steady state according to (3) when the current i is centered around zero. The unstable free response of the indenter plotted in Fig. 2 is observed when closed loop control is disabled. The coefficient K_e is determined using an unknown input observer which estimates the electromagnetic force F_{elec} produced by a given constant current i. The identified parameters used in this article are gathered in Table I.

III. Classical PID controller

The main difficulty in controlling the position of the indenter lies in its unstable dynamic behavior, dictated by the presence or absence of an oocyte against the indenter tip. Another significant difficulty is the variability of the mechanical properties of each oocyte, but especially the fact that they are unknown

TABLE I

Indenter, dummy oocyte and GeLESO parameters.

Param.	Description	Value (unit)
m	indenter mass	8.0e-6 (kg)
K_v	friction coefficient	7.32e-5 (N/m.s)
K_m	magnetic spring stiffness	-9.79e-4 (N/m)
K_e	coil electric stiffness	3.73e-7 (N/A)
K_{Oo}	dummy oocyte stiffness	[0, 0.05] (N/m)
K_m^c	target model stiffness	5e-3 (N/m)
K_v^c	target model friction coefficient	2.2e-4 (N/m.s)
w_0	GeLESO setting parameter	140

a priori. The force F_{Oo} is assumed to be roughly modeled by considering a hypothetical oocyte with a simplified elastic mechanical law. In this case, $F_{Oo} = -K_{Oo}\,d_{Oo}$, where K_{Oo} represents the elasticity of this dummy oocyte and d_{Oo} the indentation depth. The force F_{Oo} is zero when x_{id} reaches x_u and $i = 0$. Assuming that the dummy oocyte is positioned so that the contact with the indenter is established and stabilized with $F_{Oo} = 0$, the indentation depth is now defined by $d_{Oo} = x_{id} - x_u$. Such hypothetical initial conditions are impossible to meet precisely in practice. Considering this dummy oocyte correctly positioned in contact with the indenter, (3) turns into:

$$m\,\ddot{x}_{id} + K_v\,\dot{x}_{id} + \underbrace{(K_{Oo}+K_m)}_{\text{System stiffness } K}(x_{id}-x_u) = K_e\,i. \tag{4}$$

The influence of the parameter K_{Oo} on the system composed of indenter and dummy oocyte is huge. To illustrate this, the absence of the dummy oocyte corresponds to $K_{Oo} = 0$, which implies that the rigidity of the system K is equal to K_m. In this configuration, the system has two real poles $p_1 = -16.5$ and $p_2 = 7.3$, and is therefore unstable. Then, if a soft oocyte with $K_{Oo} = 0.006$ N/m is considered, then K approximates 0.005 N/m. This second configuration leads to a stable system having imaginary conjugated poles $p = -4.57 \pm 24.6i$. Finally, if a rigid oocyte with a stiffness $K_{Oo} = 0.05$ N/m is considered, the system shows two imaginary conjugated poles $p = -4.57 \pm 78.1i$, and thus, it is stable.

The image stream captured by the camera every millisecond is processed to determine the value of the measured displacement x_{id}^m of the indenter, in the vision reference frame R. The spatial resolution is 0.5 μm per pixel. The PID controller takes as input the position error $x_{ref} - x_{id}^m$, x_{ref} being a user-defined sequence of input ramps, and its output is the current i flowing through the coils. As the parameter K is unknown in practice because K_{Oo} depends on the oocyte, it is difficult to correctly tune

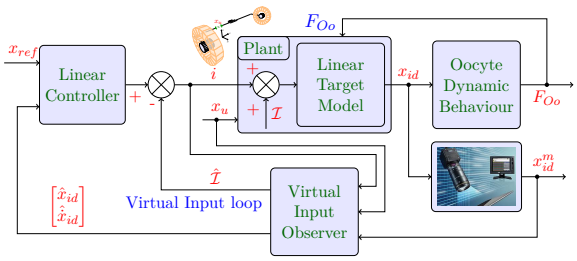

Fig. 3. Indenter position control with VIRCO: the physical system is replaced by its equivalent representation, the Virtual Input $\mathcal{I}$ rejection is done with the virtual input estimate $\hat{\mathcal{I}}$. A linear integral controller is added to cancel the steady-state error due to ramp inputs during the loading and unloading phases.

the PID coefficients so that the position error remains small during loading and unloading of the oocyte with the indenter. Several PID controller settings are also required to cope with the transition from a stable to an unstable system if the contact with oocyte is lost, and vice versa. Moreover, the mechanical behavior of an oocyte is not strictly elastic but rather viscoelastic, which can degrade the robustness of the PID controller in practice.

The quality of mechanical characterization depends directly on the tuning of the PID controller. However, it is difficult to train a clinician to correctly set the PID parameters according to the presence or absence of the oocyte. In addition, the procedure for restarting the device is complicated if the system becomes unstable due to loss of contact with the oocyte. To avoid all these drawbacks, a Virtual Input Rejection COntrol (VIRCO) has been implemented and approved to facilitate the clinician's workflow.

IV. Virtual Input Rejection COntrol

The VIRCO approach differs from traditional controller synthesis, which is based on precise mathematical modeling of the system, but instead relies on the choice of a linear model with a target behavior (see [7]). In line with (3), the target model chosen for the indenter is a second-order linear model. However, this model does not take into account the presence or absence of an oocyte and then simply corresponds to a stable mass-spring-damper model based on the identified physical parameters m, K_e and two arbitrary parameters K_v^c and K_m^c as follows:

$$m\,\ddot{x}_l + K_v^c\,\dot{x}_l + K_m^c(x_l - x_u) = K_e\,i. \qquad (5)$$

The input of this model corresponds to the current i, and its output x_l, which has no physical meaning, is homogeneous to a displacement. The coefficients K_v^c and K_m^c are determined so that the poles of this target model are $p = -13.7 \pm 20.8i$. The output x_l of the target model thus differs from the real displacement x_{id} of the indenter. The associated dynamical behavior is faster and less oscillating than those mentioned in Section III. However, using the equivalent representation theorem defined in [8], a virtual input $\mathcal{I}$ additive to the input i can be defined so that the output of the target model x_l perfectly matches the real displacement x_{id} of the indenter. The equivalent model of the indenter dynamics is therefore given by:

$$m\,\ddot{x}_{id} + K_v^c\,\dot{x}_{id} + K_m^c(x_{id} - x_u) = K_e\,(i + \mathcal{I}). \qquad (6)$$

The equivalence remains true whether the force $\vec{F}_{Oo}$ is zero or not, although the unstable behavior of the indenter has not been taken into account when defining the linear target model. Consequently, the value of the virtual input $\mathcal{I}$ depends on the evolution of the force $\vec{F}_{Oo}$, but also on all the differences in behavior between the target model and the indenter. Fig. 3 illustrates this equivalent representation principle, but also shows that if the controller is able to provide the command $-\mathcal{I}$, the dynamics of the indenter becomes strictly identical to that of the linear target model. In this ideal case, an exact global linearization of the physical system is said to be achieved, but in practice, only an estimate $\hat{\mathcal{I}}$ of the virtual input can be rejected since $\mathcal{I}$ is a mathematical construction whose exact value is unknown. The estimation process is performed using a linear unknown input observer, since the virtual input is an unknown quantity additive to the current input i, defined from a linear target model.

A. Extended state observer for Virtual Input estimation

A wide range of observers for linear systems with unknown inputs is available in the literature. In this paper, a Generic Linear Extended State Observer (GeLESO) of global order 4 is chosen to calculate $\hat{\mathcal{I}}$, estimate of $\mathcal{I}$. Its complete design and convergence proof can be found in [7]. Considering an extended state vector $X_e \in I\!R^4$, the state-space representation of (6) is stated by

$$\dot{X}_e = \mathbf{A}_e\,X_e + \mathbf{B}_e\,i + \mathcal{B}_e\,\ddot{\mathcal{I}}. \qquad (7)$$

The extended state vector X_e and the previous matrices are defined as follows

$$X_e = \begin{bmatrix} x_{id} - x_u \\ \dot{x}_{id} \\ x_3 \\ x_4 \end{bmatrix}, \quad \mathbf{A}_e = \begin{bmatrix} 0 & 1 & 0 & 0 \\ 0 & -K_v^c/m & 1 & 0 \\ 0 & -K_m^c/m & 0 & 1 \\ 0 & 0 & 0 & 0 \end{bmatrix},$$

$$\mathbf{B}_e = \begin{bmatrix} 0 \\ \frac{K_e}{m} \\ 0 \\ 0 \end{bmatrix}, \quad \mathcal{B}_e = \begin{bmatrix} 0 \\ 0 \\ 0 \\ \frac{K_e}{m} \end{bmatrix}.$$

Based on (7), the virtual input $\mathcal{I}$ is expressed as

$$\mathcal{I} = \frac{1}{K_e}(K_m^c\,(x_{id} - x_u) + m\,x_3). \qquad (8)$$

The observer state vector is thus given by

$$Z = \begin{bmatrix} \hat{x}_{id} - x_u & \hat{\dot{x}}_{id} & z_3 & z_4 \end{bmatrix}^T, \tag{9}$$

and leads to the following observer state-space representation

$$\dot{Z} = (\mathbf{A}_e - L\,C_e)Z + B_g\,U \tag{10}$$

where

$$C_e = \begin{bmatrix} 1 & 0 & 0 & 0 \end{bmatrix}, B_g = \begin{bmatrix} 0 & L_1 \\ \frac{K_e}{m} & L_2 \\ 0 & L_3 \\ 0 & L_4 \end{bmatrix}, U = \begin{bmatrix} i \\ x_{id}^m \end{bmatrix}.$$

The observer gains L_1, L_2, L_3 and L_4 in L are calculated using a single scalar parameter w_0 as follows:

$$L = \begin{bmatrix} 4w_0 & 6w_0^2 & 4w_0^3 & w_0^4 \end{bmatrix}^T.$$

The value of the virtual input estimate $\hat{\mathcal{I}}$ is therefore

$$\hat{\mathcal{I}} = \frac{1}{K_e}(K_m^c\,(\hat{x}_{id} - x_u) + m\,z_3). \tag{11}$$

The parameter w_0 is adjusted to reach a trade-off between the observer convergence speed and the estimation noise variance. It must also ensure stable closed-loop control when the virtual input estimate is rejected.

B. Indenter position control

The rejection of the virtual input allows effective control of the indenter position. The evolution of the virtual input $\mathcal{I}$ induced by slow variations in the force F_{Oo} is accurately estimated. Virtual input rejection allows the poles of the target model that control the position error $x_{ref} - \hat{x}_{id}$ to be chosen only once. A linear integral controller is also implemented to reduce the steady-state error due to ramp inputs during the loading and unloading phases. However, since the observer bandwidth is limited, the high-frequency components of $\mathcal{I}$ cannot be estimated, resulting in an approximate global linearization of the indenter dynamics.

V. Results

The image provided by the microscope vision system, annotated with the vision reference frame R can be seen in Fig. 4. The measured indenter position x_{id}^m corresponds to the coordinate along $\vec{x}$ of the small circle located at the upper left corner of the red rectangle. The measurement value is determined every millisecond by tracking the pattern inside this red rectangle. The unstable equilibrium position x_u is represented by the vertical red bar.

For each new measurement campaign with an oocyte cohort, a sterile indenter must be prepared and identified. The identification step is very important

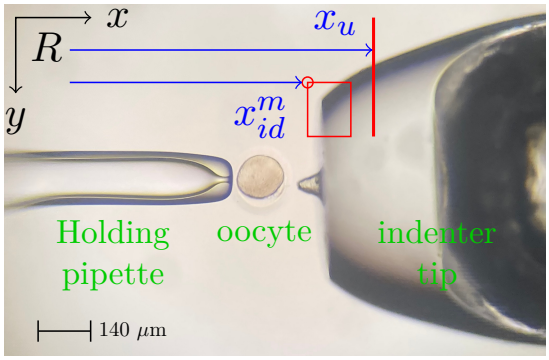

Fig. 4. Microscope view of the oocyte, the holding pipette and the indenter tip. Frame R is drawn in the upper left corner, the camera provides x_{id}^m, and the indenter unstable equilibrium position x_u linked to micropositioner position is also shown.

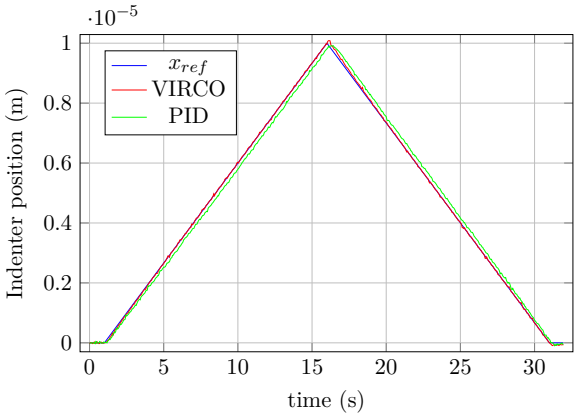

Fig. 5. Indenter position for a loading-unloading test of range 10 μm on an oocyte. Comparison of PID and VIRCO controls.

to guarantee the accuracy of the force measurement. The procedure described in Section II is very easy to follow using VIRCO. However, this procedure is inaccurate and rather tedious when performed with a PID controller. Once the system parameters have been identified, characterization of the oocyte stiffness can begin.

Considering VIRCO controller, closed-loop control is enabled and a reference value for the measured force is automatically adjusted without the oocyte to compensate for any natural drift. Then, using the holding pipette, the oocyte is placed as close as possible to the indenter tip without applying force. Once in this configuration, as the loading and unloading phases shown in Fig. 5 are automated, no further operation is required.

The process using a PID controller is quite different. Firstly, the oocyte must remain in contact with the indenter tip due to the unstable magnetic spring when the closed-loop control is activated, which inevitably leads to unwanted preload estimated to 10 nN force. Loss of contact can also occur during characterization, leading to control failure if

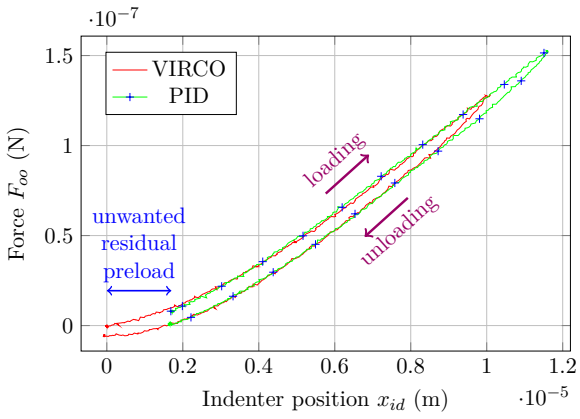

Fig. 6. Measurement of oocyte mechanical properties. Comparison of both PID and VIRCO controls on the same oocyte. Using PID control, a residual initial preload cannot be avoided prior to oocyte testing.

the preload is too low. It was also observed that a residual indentation depth of approximately 1.5 μm remains at the end, preventing the operator from visualizing how the Hertzian contact is established (see Fig. 6). For each oocyte, the operator must also iteratively adjust the PID parameters to achieve the desired performance. This process is time-consuming and must be repeated when measurement conditions change. This is the case, for instance, when loading is performed using either the sharp tip or the flat annular surface of the indenter end. This flat surface is used to test the overall behavior of the oocyte, while the sharp tip allows to characterize the local mechanical properties of the zona pellucida. The latter corresponds to the very thick and transparent outer membrane surrounding the oocyte, which plays an important role in embryo hatching a few days after oocyte fertilization. Both controllers show that the mechanical behavior of the oocyte is viscoelastic. However, VIRCO gives much better results and is easier to use for a clinician working in an assisted reproduction department.

VI. Conclusion and Perspectives

The EggSense indentation platform offers a method to characterize the mechanical properties of human oocytes while guaranteeing cell integrity. This measurement solution, which complements existing ICSI platforms, integrates seamlessly into existing IVF workflows, as the additional processing time per oocyte does not exceed 10 minutes. After oocyte retrieval, clinicians can use EggSense to measure the stiffness of each individual oocyte, thanks to a patented magnetic indentation method using low-intensity magnetic fields. This non-invasive technique could potentially provide a quantitative criterion for oocyte sorting prior to ICSI, since oocyte stiffness could be related to their level of maturity. The use of active magnetic springs coupled with the advanced VIRCO controller not only enables high-precision stiffness measurement, but also simplifies operations and reduces the associated runtime, bringing undeniable added value to the platform. To configure the controller, simply select a linear target model and implement the associated observer. This can be done once at the assembly factory and will remain unchanged for the lifetime of the equipment, regardless of the unknown mechanical properties of the cell to be characterized. EggSense is now fully operational and tested on dozen of oocyte cohorts. It has been officially approved for a clinical trial and will be integrated into ICSI programs with oocytes that will be fertilized and subsequently transferred to patients for pregnancy. The collection of a wide range of mechanical data should provide valuable insights into the distribution or statistical variability of oocyte properties.

References

[1] L. Z. Yanez, J. Han, B. B. Behr, R. A. R. era, R. A. R. Pera, and D. B. Camarillo, "Human oocyte developmental potential is predicted by mechanical properties within hours after fertilization," *Nature Communications*, vol. 7, p. 10809, 2016. [Online]. Available: https://doi.org/10.1038/ncomms10809

[2] R. Bulteau, L. Barbier, G. Lamour, Y. Lemseffer, M.-H. Verlhac, N. Tessandier, E. Labrune, M. Lenz, M.-E. Terret, and C. Campillo, "Atomic force microscopy reveals differences in mechanical properties linked to cortical structure in mouse and human oocytes," *bioRxiv*, 2025. [Online]. Available: https://www.biorxiv.org/content/early/2025/01/18/2025.01.14.632898

[3] R. Gana, J. Abadie, E. Piat, C. Roux, C. Amiot, C. Pieralli, and B. Wacogne, "A novel force sensing platform using passive magnetic springs for mechanical characterisation of human oocytes," *Sensors and Actuators A: Physical*, vol. 262, pp. 114–122, 2017. [Online]. Available: https://www.sciencedirect.com/science/article/pii/S0924424717301000

[4] S. Lamont, J. Fropier, J. Abadie, E. Piat, A. Constantinescu, C. Roux, and F. Vernerey, "Profiling oocytes with neural networks from images and mechanical data," *Journal of the Mechanical Behavior of Biomedical Materials*, vol. 138, p. 105640, 2023. [Online]. Available: https://www.sciencedirect.com/science/article/pii/S1751616122005458

[5] H. Jingqing, "Auto-disturbances-rejection controller and its applications," *Control and decision*, vol. 13, no. 1, pp. 19–23, 1998.

[6] J. Escareno, J. Abadie, E. Piat, and M. Rakotondrabe, "Robust micro-positionnig control of a 2dof piezocantilever based on an extended-state lkf," *Mechatronics*, vol. 58, pp. 82–92, 2019. [Online]. Available: https://www.sciencedirect.com/science/article/pii/S0957415819300133

[7] F. Amokrane, E. Piat, J. Abadie, A. Drouot, and J. Escareno, "State observation of unknown nonlinear siso systems based on virtual input estimation," *International Journal of Control*, vol. 94, no. 7, pp. 1838–1851, 2019. [Online]. Available: https://doi.org/10.1080/00207179.2019.1680869

[8] S. Hernandez, E. Piat, J. Abadie, and E. Lesniewska, "Unknown input uncertainty calculation using virtual input shaping and interval analysis," *Measurement*, vol. 243, p. 116140, 2025. [Online]. Available: https://www.sciencedirect.com/science/article/pii/S0263224124020256

[9] E. Piat, J. Abadie, and S. Oster, "Nanoforce estimation based on kalman filtering and applied to a force sensor using diamagnetic levitation," *Sensors and Actuators A: Physical*, vol. 179, pp. 223–236, 2012. [Online]. Available: https://www.sciencedirect.com/science/article/pii/S0924424712001288